Demographic inference using the SFS with `moments` and `demes`

Nick Collier[1] and Aaron P. Ragsdale[1,*]

[1]Department of Integrative Biology, University of Wisconsin–Madison
[*]apragsdale@wisc.edu

March 31, 2025

Abstract

In this chapter we show how to use `moments`, a Python package for computing the joint SFS and inferring demographic history, through its `demes` interface. Following a discussion of SFS inference, we illustrate the general usage of `moments` and sketch two specific examples. We conclude with a discussion of some additional considerations regarding the `moments` library.

Introduction

The genetic composition of a sample of individuals is shaped by their genome biology and evolutionary history. Variation resulting from this history can be fully represented by the ancestral relationships among samples at each locus in the genome and how those gene-genealogical relationships change along a chromosome due to recombination (that is, by information stored in the Ancestral Recombination Graph (Nielsen et al., 2025)). However, the ARG can be large and unwieldy, and methods for reconstructing history directly from the ARG, while showing promise (e.g., YC Brandt et al., 2022; Fan et al., 2023; Brandt et al., 2024), are in their infancy and so far limited in application and scalability. Instead, evolutionary inference using informative summaries of genetic variation remains a tractable and powerful alternative for learning parameters of population history, natural selection and genome biology.

One such summary that has seen wide use is the site frequency spectrum (SFS), which stores the counts (observed or expected) of alleles carried by a given number of genomes in a set of samples. Like any summary of the data, the SFS discards some information stored in the ARG – in this case, loci are treated independently so that haplotypic information is lost. Even so, the relative densities of allele frequencies and the overall scale of the SFS are both sensitive to demographic and non-demographic processes.

This chapter focuses on multi-population demographic inference from the SFS using `moments` (Jouganous et al., 2017). Past population processes, including changes in population size, splits, gene flow and population structure, impact the SFS in predictable ways. A population size expansion (or contraction) leads to a relative excess (or deficit) of low-frequency variants, for example, and commonly used statistics measuring population divergence, such as F_{ST}, are themselves summaries of the SFS. Thus, the development of methods to learn demographic history from the SFS came soon after the publication of whole-genome sequencing from multiple individuals (Marth et al., 2004; Williamson et al., 2005). More recent methodological advances allow for increased sample sizes and numbers of populations, providing a rich ecosystem of software for SFS-based demographic inference (Gutenkunst et al., 2009; Excoffier and Foll, 2011; Gravel et al., 2011; Jouganous et al., 2017; Ragsdale et al., 2018; Kamm et al., 2020; Dilber and Terhorst, 2024). We return to this in the final section: Considerations and Caveats.

Other evolutionary mechanisms are known to affect allele frequency dynamics and the SFS. This presents a challenge for demographic inference, as the observed SFS may be distorted by non-demographic processes. However, this also presents an opportunity to learn about different evolutionary processes, if demographic

history can be controlled for. The SFS has been used to infer the distribution of fitness effects of new mutations, primarily for nonsynonymous variation in coding regions (e.g., Eyre-Walker et al., 2006; Boyko et al., 2008; Kim et al., 2017); to scan for historical selective sweeps (e.g., Kim and Stephan, 2002; Nielsen et al., 2005); and to understand how selection on quantitative traits impacts the genetic architecture underlying those traits (eg., Patel et al., 2024; Ragsdale, 2024). The SFS has also been used to infer relative mutation rates and how they have changed over time (DeWitt et al., 2021). Each of these analyses typically requires partitioning the data in some way – by functional annotation, mutation context, local recombination rate, etc – so that comparisons can be made across SFS from different classes of mutations.

Interfacing `moments` with `demes`

Specifying demographic models requires defining populations (or "demes") and their relationships via splits and gene flow. `demes` provides a standardized and accessible format for defining demographic models (Gower et al., 2022), and has been adopted by widely used software for population genetics simulation and inference (including `msprime` (Baumdicker et al., 2022), `momi` (Dilber and Terhorst, 2024), `fwdpy11` (Thornton, 2019), `GADMA` (Noskova et al., 2023)). `demes` encourages interoperability and reuse of code across software, ease of model implementation and reduction of errors.

Demographic models are specified in YAML format (see Gower et al. (2022) and the associated documentation). The two-population split-with-migration model depicted in Figure 1A is specified as below:

```yaml
description: split-with-migration model, loosely based on example 2
generation_time: 29
time_units: years
demes:
- name: ancestral
  epochs:
  - {start_size: 15000, end_time: 300000}
  - {start_size: 25000, end_time: 75000}
- name: popA
  ancestors: [ancestral]
  epochs:
  - {start_size: 30000}
- name: popB
  ancestors: [ancestral]
  epochs:
  - {start_size: 1200, end_size: 14000}
migrations:
- demes: [popA, popB]
  rate: 5e-5
```

In `moments`, a `demes`-specified demographic model can be directly used to compute either the SFS or multi-population LD statistics (Ragsdale and Gravel, 2019, 2020). For the SFS, we simply need to load the demographic model using `demes` and specify the number of haploid samples to draw and from which populations.

```python
import demes, moments
g = demes.load('model.yaml')
samples = {'popA': 60, 'popB': 60}
fs = moments.Demes.SFS(g, samples=samples)
```

Here, we have not specified a mutation rate. The default behavior sets $u = 1$, so that $\theta = 4N_e u = 4N_e$, where N_e is the ancestral population's initial size. With a known mutation rate, the SFS will be properly
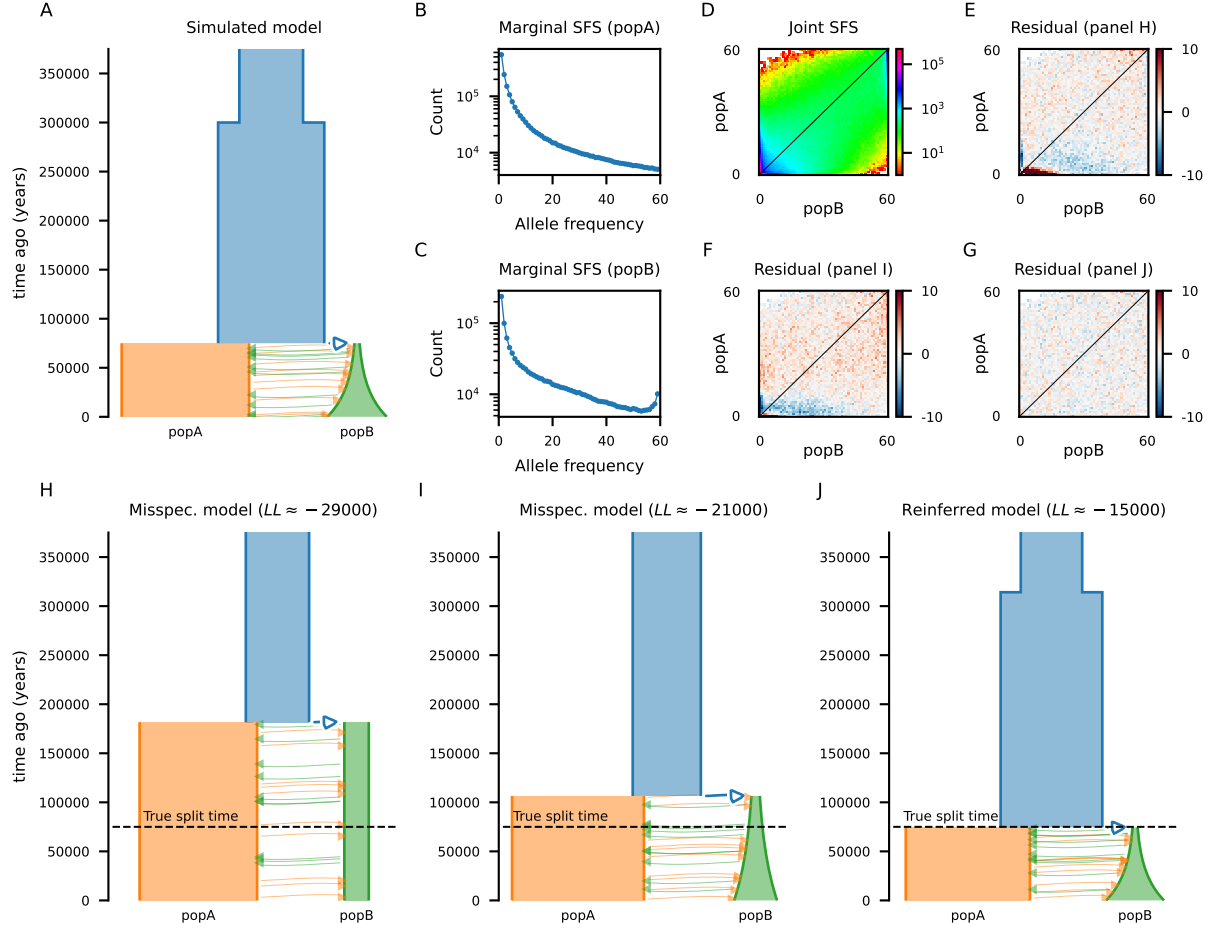
Figure 1: Caption placeholder

scaled by passing the mutation rate as a keyword argument: `moments.Demes.SFS(g, samples=samples, u=u)`. This is equivalent to scaling the output SFS above by multiplying by `u`, as `u*fs`.

Examples: inference in `moments` using `demes`

Below, we show two examples of multi-population demographic inference using the joint SFS. The first example simulates data with known demographic parameters, which we try to reinfer using the both the original model and simpler misspecified ones. In the second example, we infer a relatively simple human-Neanderthal history using data from two human populations and a high-coverage ancient sample from the Neanderthal lineage. For both of these examples, we briefly describe data processing and inference setup, emphasizing the high-level components of the analyses. For detailed information about each example, including managing data, specifying models, performing inference, computing confidence intervals and visualizing fits, we refer readers to the accompanying GitHub repository (`https://github.com/StatisticalPopulationGenomics-2ndEd/moments`), which is maintained with up-to-date versioning.

In order to optimize parameters in a `demes` model, we need a way to specify which parameters should be fit. For this, we use a separate YAML-formatted file to define `parameters`, each of which points to desired value(s) in the demographic model and sets lower and upper bounds. This file also specifies any relative

`constraints` between pairs of parameters, to ensure the optimization routine only explores valid model space. Below, we have included a truncated parameters file – the full example is available on GitHub.

```yaml
parameters:
- name: T0
  values:
  - demes:
      ancestral:
        epochs:
          0: end_time
  lower_bound: 0
  upper_bound: 2e5
- name: T1
  values:
  - demes:
      ancestral:
        epochs:
          1: end_time
  lower_bound: 0
  upper_bound: 1e6
- name: Ne
  values:
  - demes:
      ancestral:
        epochs:
          0: start_size
  lower_bound: 1e2
  upper_bound: 1e6
...
constraints:
- params: [T0, T1]
  constraint: greater_than
```

Taking the demographic model, parameters file, and observed SFS together, we can perform inference using the `moments.Demes.Inference.optimize(...)` function. The initial parameter guesses are given by the input demographic model, which may be perturbed using a keyword argument. Any value in the demographic model that is not specified in the parameters file will remain unchanged, and is therefore treated as a fixed parameter. Here, we also assume we have an estimate for the total mutation rate, U.

```python
import moments

data = moments.Spectrum.from_file('data.fs')
U = 1e-8 * 5e8  # per-base mutation rate times the total length

model_file = 'model.yaml'
params_file = 'params.yaml'
output = 'model.fit.yaml'

ret = moments.Demes.Inference.optimize(
    model_file, params_file, data,
    perturb=1, uL=U, output=output
)
```

Confidence intervals may also be computed using `moments.Demes.Inference.uncerts(...)`, once a (locally) optimal model has been found. The following will emit a tab-separated file containing parameter names, best-fit values and estimated standard errors.

```
log_file = 'log.txt'

uncerts = moments.Demes.Inference.uncerts(
  output, params_file, data,
  uL=U, output=log_file
)
```

Inferring parameters in a simulated split-with-migration model

Using the split-with-migration model defined above (illustrated in Figure 1A), we simulated data for 30 diploid individuals from both populations using `msprime` (Baumdicker et al., 2022). These simulations consided of 500 regions, each of length 1 Mb, with per-base recombination and mutation rates of 10^{-8}. The joint SFS was computed using `tskit`'s `ts.allele_frequency_spectrum()` function separately on each replicate region and summing across regions to find the total SFS across 500 Mb of data (Figure 1B–D).

We fit three demographic models to the simulated data. In addition to reinferring the parameters from the simulated model, we fit two simpler models to the same data. These had fewer parameters, both omitting the size change deeper in time in the ancestral population. This is meant to crudely mimic the scenario that we often face, in which the true history is more complicated than the parameterized model. It also highlights biases in inferences that can arise when features of the true history are not included.

When fitting the two misspecified models that do not allow for size changes in the ancestral population, this split time is inferred to be substantially deeper in the past than the true split time. This effect, as demonstrated by **?**, is due to the decreased coalescence rate within the ancestral population between the time of the expansion and divergence of the descendent populations. These two misspecified models (Figure 1H,I) also provide a worse fit to the data, as seen by the lower log-likelihoods and the large residuals between model predictions and data (Figure 1E-G).

Inferring human-Neanderthal demographic parameters

We obtained modern human genome sequences from a recent resequencing of the 1000 Genomes Project cohort (Byrska-Bishop et al., 2022), and used the high-coverage sequence of the Vindija Neandertal from Prüfer et al. (2017). From the 1000 Genomes cohort we took 85 MSL (Mende from Sierre Leone) and 91 GBR (British from England and Scotland) sequences as our modern human samples. We filtered out sites that lay outside the 1000 Genomes 'strict' mask, were not genotyped in all four existing high-coverage archaic genome sequences, thatlacked high-confidence ancestral state assignments, or fell within 10 kb of exonic or promoter regions and were left with approximately 960 Mb of well-characterized and putatively neutrally-evolving sequence. We estimated the genome-wide SFS using built-in `moments` parsing functions. Details concerning data processing (including our liftover of the Vindija sequence to a more recent genome build) can be found in the linked GitHub repository.

The model that we wished to fit is relatively simple but still has many parameters (11 in the example we present), so we constructed it in stages by first fitting simpler one– and two–population models. Throughout, we used $u = 1.5 \cdot 10^{-8}$ as an estimate of the mutation rate per generation and 29 years as the average generation time. We began by fitting one-population models with ancestral and recent size changes for MSL and GBR. For the MSL model, we allowed three epochs with constant effective size in each epoch. We attributed to GBR a sharp contraction ∼60 kya followed by exponential growth to represent the out-of-Africa bottleneck and subsequent rapid expansion. YAML files representing the models and parameters in this section can be found in the linked GitHub repository.

We next stitched these one-population models together and refitted the resulting graph to get a two-population model that included continuous symmetric migration between MSL and GBR and an ancestral

size expansion. Following this, we added a Neandertal branch and fitted the Neandertal-modern human divergence time, Neandertal effective size, and the Neandertal-to-GBR admixture proportion. We also fitted the divergence time between the sampled Vindija Neandertal lineage and the Neandertal lineage which admixed with modern non-African humans. Finding that this parameter tended to converge to its lower bound (imposed by the estimated time of death of the Vindija Neandertal, 55 kya), we fixed it to a value supported by literature (90 kya, Prüfer et al. (2017)) in a second round of optimization. Rather than fitting it, we fixed the time of the Neandertal-GBR pulse to 50 kya. Fixing parameters for which good estimates are available in the literature (see e.g. Sümer et al. (2025)) may be reasonable in the first stages of model optimization, and we expected this value to be especially difficult to fit due to the small pulse proportion and Neandertal sample size. In the second round of optimization on the three-population model, we refit all parameters aside from the two event times mentioned above to refine the estimates.

After this refitting step, we were left with parameters in good agreement with prior authors, with a Neandertal-modern human divergence time of 547 kya, MSL-GBR split time of 77 kya, and Neandertal-GBR pulse proportion of 2.7 percent. We observe some large residuals in our best-fit model Figure 2G-I), suggesting ...

Considerations and caveats

1. Include here general ideas about the strengths and weaknesses of various approaches in population genetic inference, including when using the SFS.

2. Challenges in finding local/global optima.

3. Challenges in exploring parameter space.

4. Background selection [Ewing, Johri]

5. Gene dense vs gene sparse genomic architectures among species.

References

Franz Baumdicker, Gertjan Bisschop, Daniel Goldstein, Graham Gower, Aaron P Ragsdale, Georgia Tsambos, Sha Zhu, Bjarki Eldon, E Castedo Ellerman, Jared G Galloway, et al. Efficient ancestry and mutation simulation with msprime 1.0. *Genetics*, 220(3):iyab229, 2022.

Adam R Boyko, Scott H Williamson, Amit R Indap, Jeremiah D Degenhardt, Ryan D Hernandez, Kirk E Lohmueller, Mark D Adams, Steffen Schmidt, John J Sninsky, Shamil R Sunyaev, et al. Assessing the evolutionary impact of amino acid mutations in the human genome. *PLoS genetics*, 4(5):e1000083, 2008.

Débora YC Brandt, Christian D Huber, Charleston WK Chiang, and Diego Ortega-Del Vecchyo. The promise of inferring the past using the ancestral recombination graph. *Genome biology and evolution*, 16 (2):evae005, 2024.

Marta Byrska-Bishop, Uday S Evani, Xuefang Zhao, Anna O Basile, Haley J Abel, Allison A Regier, André Corvelo, Wayne E Clarke, Rajeeva Musunuri, Kshithija Nagulapalli, et al. High-coverage whole-genome sequencing of the expanded 1000 genomes project cohort including 602 trios. *Cell*, 185(18):3426–3440, 2022.

William S DeWitt, Kameron Decker Harris, Aaron P Ragsdale, and Kelley Harris. Nonparametric coalescent inference of mutation spectrum history and demography. *Proceedings of the National Academy of Sciences*, 118(21):e2013798118, 2021.

Enes Dilber and Jonathan Terhorst. Faster inference of complex demographic models from large allele frequency spectra. *bioRxiv*, 2024.
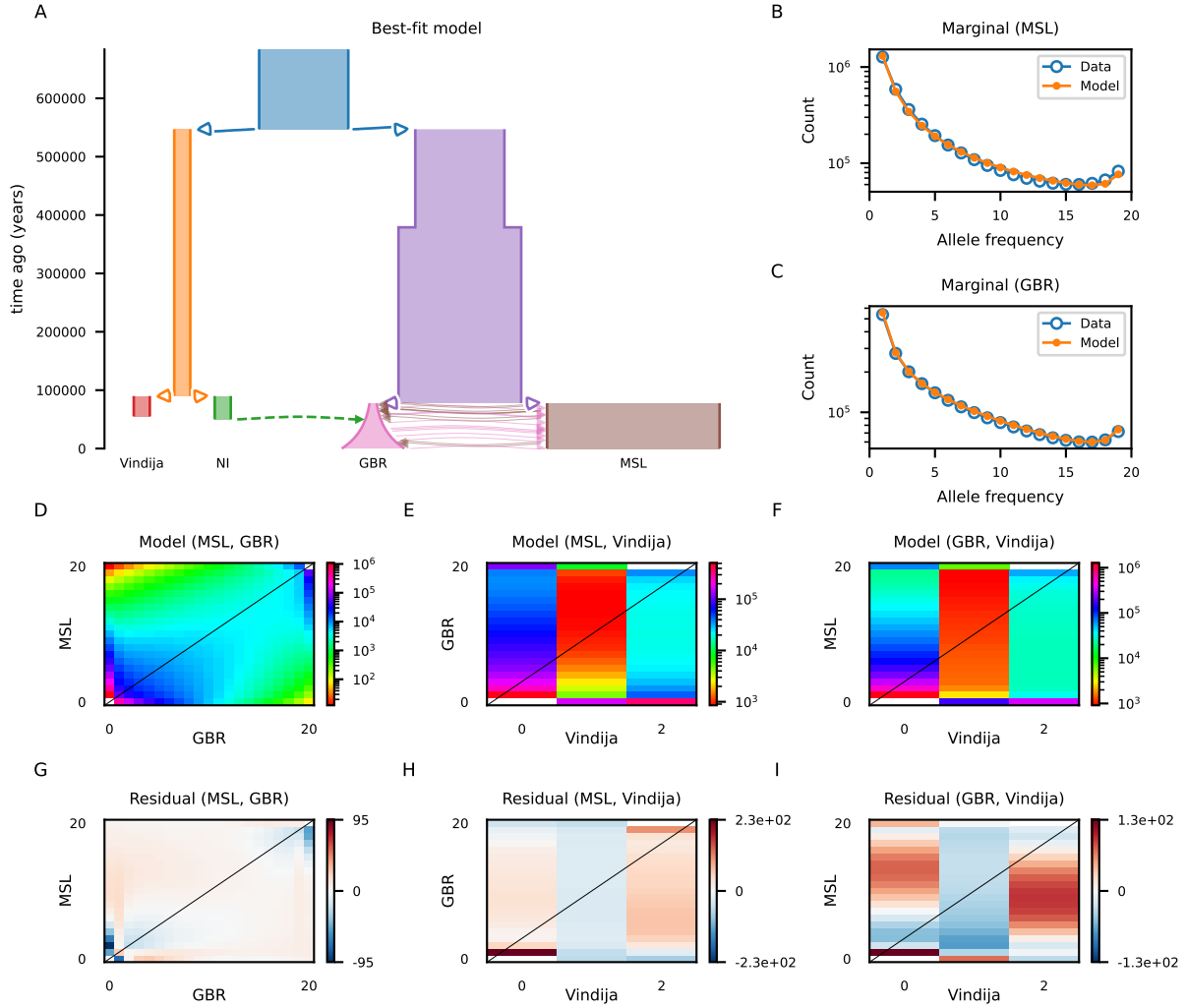
Figure 2: A plot of the best-fit model created using `demesdraw` is displayed in (A). Marginal SFS fits between the model and empirical data are shown for MSL (B) and GBR (C). Marginal two-way spectra predicted by the model and their residuals against the data are plotted for the three pairs of populations MSL, GBR (D and G), MSL, Vindija (E and H), and GBR, Vindija (F, I).

Laurent Excoffier and Matthieu Foll. Fastsimcoal: a continuous-time coalescent simulator of genomic diversity under arbitrarily complex evolutionary scenarios. *Bioinformatics*, 27(9):1332–1334, 2011.

Adam Eyre-Walker, Megan Woolfit, and Ted Phelps. The distribution of fitness effects of new deleterious amino acid mutations in humans. *Genetics*, 173(2):891–900, 2006.

Caoqi Fan, Jordan L Cahoon, Bryan L Dinh, Diego Ortega-Del Vecchyo, Christian Huber, Michael D Edge, Nicholas Mancuso, and Charleston WK Chiang. A likelihood-based framework for demographic inference from genealogical trees. *bioRxiv*, 2023.

Graham Gower, Aaron P Ragsdale, Gertjan Bisschop, Ryan N Gutenkunst, Matthew Hartfield, Ekaterina Noskova, Stephan Schiffels, Travis J Struck, Jerome Kelleher, and Kevin R Thornton. Demes: a standard format for demographic models. *Genetics*, 222(3):iyac131, 2022.

Simon Gravel, Brenna M Henn, Ryan N Gutenkunst, Amit R Indap, Gabor T Marth, Andrew G Clark, Fuli Yu, Richard A Gibbs, 1000 Genomes Project, Carlos D Bustamante, et al. Demographic history and rare allele sharing among human populations. *Proceedings of the National Academy of Sciences*, 108(29): 11983–11988, 2011.

Ryan N Gutenkunst, Ryan D Hernandez, Scott H Williamson, and Carlos D Bustamante. Inferring the joint demographic history of multiple populations from multidimensional snp frequency data. *PLoS genetics*, 5 (10):e1000695, 2009.

Julien Jouganous, Will Long, Aaron P Ragsdale, and Simon Gravel. Inferring the joint demographic history of multiple populations: beyond the diffusion approximation. *Genetics*, 206(3):1549–1567, 2017.

Jack Kamm, Jonathan Terhorst, Richard Durbin, and Yun S Song. Efficiently inferring the demographic history of many populations with allele count data. *Journal of the American Statistical Association*, 115 (531):1472–1487, 2020.

Bernard Y Kim, Christian D Huber, and Kirk E Lohmueller. Inference of the distribution of selection coefficients for new nonsynonymous mutations using large samples. *Genetics*, 206(1):345–361, 2017.

Yuseob Kim and Wolfgang Stephan. Detecting a local signature of genetic hitchhiking along a recombining chromosome. *Genetics*, 160(2):765–777, 2002.

Gabor T Marth, Eva Czabarka, Janos Murvai, and Stephen T Sherry. The allele frequency spectrum in genome-wide human variation data reveals signals of differential demographic history in three large world populations. *Genetics*, 166(1):351–372, 2004.

Rasmus Nielsen, Scott Williamson, Yuseob Kim, Melissa J Hubisz, Andrew G Clark, and Carlos Bustamante. Genomic scans for selective sweeps using snp data. *Genome research*, 15(11):1566–1575, 2005.

Rasmus Nielsen, Andrew H Vaughn, and Yun Deng. Inference and applications of ancestral recombination graphs. *Nature Reviews Genetics*, 26(1):47–58, 2025.

Ekaterina Noskova, Nikita Abramov, Stanislav Iliutkin, Anton Sidorin, Pavel Dobrynin, and Vladimir I Ulyantsev. Gadma2: more efficient and flexible demographic inference from genetic data. *GigaScience*, 12:giad059, 2023.

Roshni A Patel, Clemens L Weiß, Huisheng Zhu, Hakhamanesh Mostafavi, Yuval B Simons, Jeffrey P Spence, and Jonathan K Pritchard. Conditional frequency spectra as a tool for studying selection on complex traits in biobanks. *bioRxiv*, 2024.

Kay Prüfer, Cesare De Filippo, Steffi Grote, Fabrizio Mafessoni, Petra Korlević, Mateja Hajdinjak, Benjamin Vernot, Laurits Skov, Pinghsun Hsieh, Stéphane Peyrégne, et al. A high-coverage neandertal genome from vindija cave in croatia. *Science*, 358(6363):655–658, 2017.

Aaron P Ragsdale. Archaic introgression and the distribution of shared variation under stabilizing selection. *bioRxiv*, pages 2024–08, 2024.

Aaron P Ragsdale and Simon Gravel. Models of archaic admixture and recent history from two-locus statistics. *PLoS genetics*, 15(6):e1008204, 2019.

Aaron P Ragsdale and Simon Gravel. Unbiased estimation of linkage disequilibrium from unphased data. *Molecular Biology and Evolution*, 37(3):923–932, 2020.

Aaron P Ragsdale, Claudia Moreau, and Simon Gravel. Genomic inference using diffusion models and the allele frequency spectrum. *Current Opinion in Genetics & Development*, 53:140–147, 2018.

Arev P Sümer, Hélène Rougier, Vanessa Villalba-Mouco, Yilei Huang, Leonardo NM Iasi, Elena Essel, Alba Bossoms Mesa, Anja Furtwaengler, Stéphane Peyrégne, Cesare de Filippo, et al. Earliest modern human genomes constrain timing of neanderthal admixture. *Nature*, 638(8051):711–717, 2025.

Kevin R Thornton. Polygenic adaptation to an environmental shift: temporal dynamics of variation under gaussian stabilizing selection and additive effects on a single trait. *Genetics*, 213(4):1513–1530, 2019.

Scott H Williamson, Ryan Hernandez, Adi Fledel-Alon, Lan Zhu, Rasmus Nielsen, and Carlos D Bustamante. Simultaneous inference of selection and population growth from patterns of variation in the human genome. *Proceedings of the National Academy of Sciences*, 102(22):7882–7887, 2005.

Débora YC Brandt, Xinzhu Wei, Yun Deng, Andrew H Vaughn, and Rasmus Nielsen. Evaluation of methods for estimating coalescence times using ancestral recombination graphs. *Genetics*, 221(1):iyac044, 2022.